ISSN1027-5495. Functional Materials, 31, No.4 (2024), p. 638-645
doi:http://dx.doi.org/10.15407/fm31.04.638

Synthesis and adsorption performance of Cu-BTC microspheres for Methylene Blue Dye

Fei Lu, Qi Guan

School of Chemistry and Pharmaceutical Engineering, Jilin Institute of Chemical Technology, Jilin 132022, P. R. China

Received September 20, 2024

The MOFs, copper–1,3,5- benzenetricarboxylate (Cu-BTC) samples were synthesized by immersing self-assembled films in solutions of copper nitrate and trimesic acid through a biomimetic mineralization method. During the synthesis, self-assembled monolayers with different end groups acted as templates, facilitating the nucleation and growth of Cu-BTC crystals. The resulting products were characterized using scanning electron microscopy (SEM), Fourier transform infrared spectroscopy (FTIR), and Brunauer-Emmett-Teller (BET) analysis. The influence of the synthesized materials on the adsorption performance of methylene blue (MB) dye was systematically investigated. The results show that the Cu-BTC compound microspheres, induced by sulfonic acid groups, have a uniform morphology and exhibit effective adsorption of MB dye. The theoretical maximum adsorption capacity of these microspheres for MB dye is 75.6 mg $\cdot g^{-1}$. The adsorption data from this process are consistent with both the pseudo-first-order kinetic model and the Langmuir isotherm model. After four adsorption-regeneration cycles, the microspheres retained a high adsorption efficiency for MB dye.

Keywords: Self-assembled films, Cu-BTC, bionic mineralization; adsorption; methylene blue

Синтез та адсорбційні характеристики мікросфер Cu-BTC для барвника метиленового синього. *Fei Lu, Qi Guan* Зразки MOFs, міді-1,3,5- бензолтрикарбоксилату (Cu-BTC) були синтезовані шляхом занурення самоорганізованих плівок у розчини нітрату міді та тримезинової кислоти методом біоміметичної мінералізації. Під час синтезу самозбірні моношари з різними кінцевими групами діяли як матриці, сприяючи зародженню та зростанню кристалів Cu-BTC. Отримані продукти були охарактеризовані за допомогою скануючої електронної мікроскопії (SEM), інфрачервоної спектроскопії з перетворенням Фур'є (FTIR) та аналізу Брунауера-Еммета-Теллера (BET). Було систематично досліджено вплив синтезованих матеріалів на адсорбційні властивості барвника метиленового синього (MB). Результати показують, що мікросфери сполуки Cu-BTC, індуковані групами сульфокислоти, мають однакову морфологію та демонструють ефективну адсорбцію барвника MB. Теоретична максимальна адсорбційна здатність цих мікросфер для барвника MB становить 75,6 мг т–1. Дані про адсорбцію цього процесу узгоджуються як з кінетичною моделлю **псевдопершого порядку, так і з моделлю ізотерми Ленгмюра.** Після чотирьох циклів адсорбції-регенерації мікросфери зберегли високу адсорбційну ефективність для барвника MB

1. Introduction

Synthetic organic dyes are cheap and provide a wide range of colors, which are widely used in the paper-making, leather tanning, pharmaceutical, photography, and cosmetics industries [1-2]. Unfortunately, dyes are highly toxic and can cause cancer and mutagenic effects even at low concentrations in organisms. Due to their high chemical stability, removing dyes from water is a challenging problem [2].

Many methods have been proposed to remove dyes from wastewater, such as electrochemical degradation, membrane separation, ultra filtration and extraction [3, 4]. The above methods that have many advantages cannot be applied on a large scale due to high costs, generation of secondary pollution, and waste generation [5]. Adsorption, applicable to virtually all types of dyes or dye mixtures, is an effective method for dye removal that offers a number of significant advantages. The adsorption method does not require specialized equipment or pretreatment and can be repeated multiple times until the adsorbent reaches its maximum adsorption capacity. Polycrystalline Cu-BTC, a metal-organic framework material composed of copper and its organic ligand 1,3,5-benzenetricarboxylic acid (BTC), which exists in the form of spherical crystals or polycrystalline powder, has gradually become a research hotspot in dye wastewater treatment due to its high porosity and surface area [6-7]. There are many different preparation methods for preparing metal-organic frameworks (MOFs) materials, including solvent, heat treatment, hydrothermal method, ultrasonic method, ion exchange method, vapor phase deposition method, etc. [8]. The appropriate pore size and morphology of MOFs play a key role. On the other hand, MOFs with too small pores can prevent large-sized reactant molecules, product molecules, and reaction intermediates from entering or exiting the pores easily. Meanwhile, MOFs also hinder the rapid diffusion and transport of small molecules within the pores after entering the pores. This greatly limits the practical application of MOFs. It is important to adjust the pore size of MOFs according to actual needs [9]. Biomineralization, as an emerging preparation method, has attracted much attention due to its advantages such as mild reaction conditions and adjustable pore structure [10].

In our previous studies, we have shown that the growth of materials can be controlled using biomineralization technology [11–12]. In this study, we successfully employed biomineralization technology to control the morphology and pore size of Cu-BTC, resulting in micron-sized spherical samples. Subsequently, the adsorption capacity of spherical Cu-BTC as an adsorbent for methylene blue was studied.

2. Experimental

The ITO conductive glasses were soaked in Piranha solution (a 7:3 volume ratio of H_2SO_4 to H_2O_2) at 90°C for 30 minutes to produce hydroxyl radicals on their surfaces. Part of the obtained substrate with hydroxyl groups serves as a template for hydroxyl substrate, while on the other hand, according to literature data, self-assembled monolayers with thiol, amino and sulfonic acid groups are prepared [12].

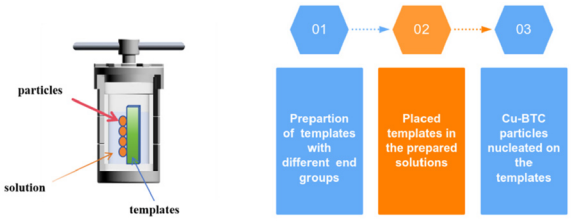

Fig 1. Experimental process diagram

The Cu-BTC materials were synthesized as follows. First, solution A was prepared by dissolving 1.093 g of copper nitrate trihydrate in 15 mL of deionized water with stirring. Next, solution B was prepared by dissolving 0.525 g of trimesic acid in 15 mL of ethanol, also under stirring. Subsequently, solution A was added to solution B and mixed thoroughly. The resulting mixture was placed in a hydrothermal reactor, and the substrates modified with self-assembled monolayers (SAMs) and hydroxyl substrate were vertically inserted into the above solution. The blue Cu-BTC powders were obtained on the surface of SAM-modified substrates and hydroxyl substrates at 120°C for 12 hours. Fig.1 illustrates the experimental process. The obtained samples were soaked in ethanol for 48 hours, with the ethanol being changed every 12 hours to remove agents and other impurities.

Functional groups of the samples were determined using a Perkin-Elmer 550s model spectrophotometer with a scanning range of 4000 to 400 cm^{-1}. The morphology and surface structure of MOFs materials were observed using a scanning electron microscope (SEM) JSM-6710F produced by JEOL Co., Ltd. The specific surface area and pore volume of the MOFs materials were tested and analyzed using an ASAP 2020 model N_2 physical adsorption instrument from Micromeritics Instrument Corporation.

To investigate the adsorption performance of Cu-BTC for MB, we analyzed the influence of initial solution pH, contact time, and initial MB concentration. Specifically, 20mg of Cu-BTC was added to a 40mL MB solution with varying concentrations. The suspension was then shaken at 180r min^{-1} for a specific duration under controlled conditions at 25°C. Subsequently,

the upper layer solution was filtered through a 0.45μm filter and the mass concentration of MB in the adsorption equilibrium state was determined using a UV-visible spectrophotometer at 664nm.

3. Results and discussion

Fig.2 presents the infrared absorption spectra for each sample. It is evident that the position of the infrared absorption peak for the spontaneously generated sample closely aligns with that of the template-induced sample. The absorption peaks at 730 cm^{-1} and 762 cm^{-1} are attributed to the bending vibrations of C-H bonds, while the peaks at 1370 cm^{-1} and 1632 cm^{-1} correspond to the symmetric and asymmetric stretching vibrations of the C=O bond in carboxylate groups. Notably, no characteristic peak for COOH is observed at 1700 cm^{-1}, indicating that Cu^{2+} ions reacted with H_3BTC to form Cu-BTC. The peak at 3500 cm^{-1} is associated with the presence of crystal water in Cu-BTC crystals [13]. The results of the study show that the incorporation of a template in the experimental procedure does not modify the structure of the Cu-BTC sample.

The SEM images in Fig. 3a and 3f illustrate the formation of an octahedral structure in the absence of template that is largely consistent with those reported in the literature [14–15]. SEM images in Fig. 3b show that octahedra of Cu-BTC were formed on hydroxyl substrates. The size of the samples (Fig.3b) is larger than that of natural formed samples [16]. The SEM image in Fig.3c demonstrates that on modified SAM substrates with terminal amino groups, various polyhedral shapes such as spheres, tetrahedrons and hexagons of Cu-BTC granules appear. On thiol-terminated SAM substrates, the morphology resembles closely spaced spherical structures (Fig. 3d). Similarly, Fig. 3e shows irregular spheres of Cu-BTC which appeared on the modified sulfone-terminated SAM substrates. Compared to Fig 3d, the spheres in Fig. 3e are not connected to each other but exist independently.

It is widely acknowledged that electrostatic interactions, lattice geometric matching, stereochemical matching, hydrogen bonding, etc., are significant factors influencing the nucleation and growth of crystals induced by organic membranes [17]. In our experiments, the electronegativity sequence of these four functional groups was as follows: sulfonic

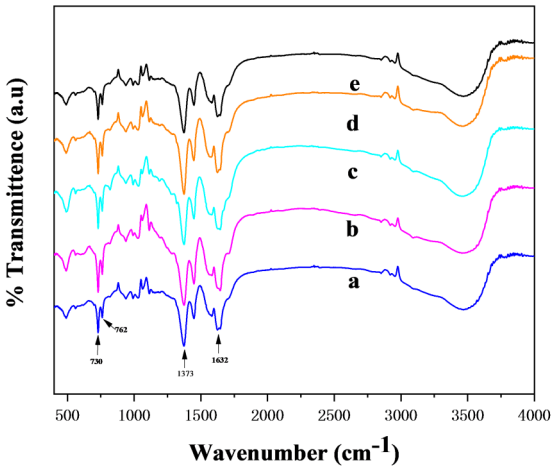

Fig. 2. FTIR spectra of Cu-BTC microcrystal grown on the SAM template with the ending groups (a) blank;(b) hydroxyl-group; (c) amino group; (d) thiol group; (e) sulfonic group.

group > hydroxyl group > amino group > thiol group. The order of the hydrogen bonding effect was: hydroxyl group > amino group > sulfonic group > thiol group. Therefore, hydroxyl and amino groups combined with the substrate via hydrogen bonding and trimesic acid, giving the surface a negative charge. Meanwhile, the sulfonic group mainly bonded to copper ions through electrostatic interaction, resulting in a positive surface charge of the substrate. On the whole the sequence in which various terminal templates attract negative ions is the sulfonic group > thiol group > amino group > hydroxyl group. From a general point of view, in accordance with the law of crystal growth [18], crystal nuclei with lower free energy and spherical morphology initially arise in the system. However, under the influence of crystallization kinetic factors they are transformed into other morphologies. Since Cu-BTC is an anionic MOF material, the electrostatic attraction can prevent the transformation of spherical crystal nuclei into crystals of other morphologies. Furthermore, during the crystal growth, the surface energy of crystal faces is related to the supersaturation of crystal growth units in the reaction system. An increase in the supersaturation of crystal growth units results in the appearance of crystal faces with higher surface energy. In the absence of a template, Cu^{2+} and BTC^{3-} can react directly, thus the crystal growth units of Cu-BTC are readily formed, and the degree of supersaturation of the crystal growth units is relatively high. Hence, polyhedra with high surface energy can be formed. The negatively charged substrate can be adsorbed on the sur-

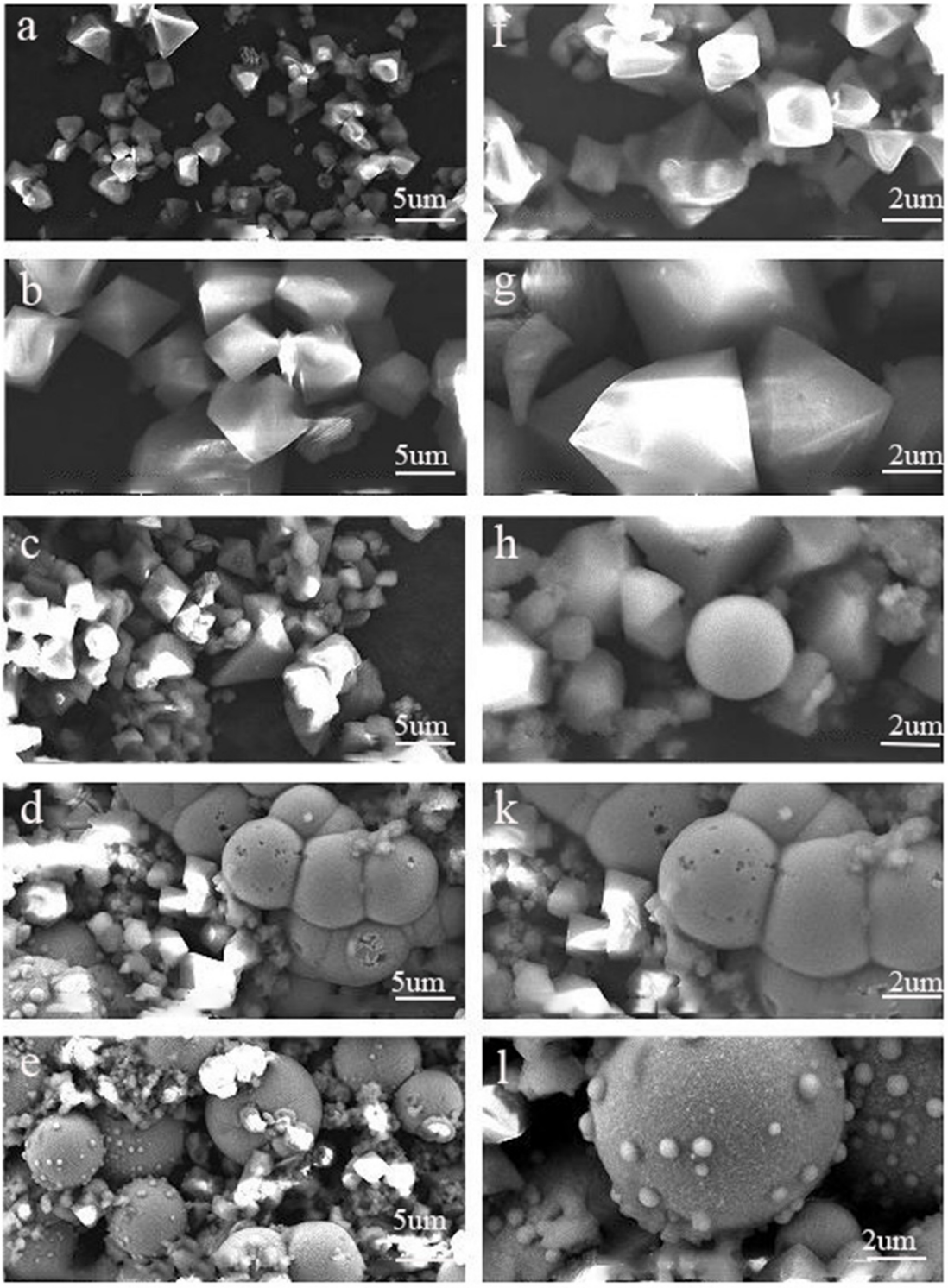

Fig. 3. SEM images of Cu-BTC microcrystal grown on the SAMs template with the ending groups (a) blank;(b) hydroxyl-group; (c) amino group; (d) thiol group; (e) sulfonic group; (f, g, h,k,l) the corresponding larger versions of (a,b, c, d,e)

face of the ligand ions (BTC^{3-}); this can prevent the formation of crystal growth units and subsequently reduce the degree of supersaturation of the crystal growth units, resulting in the formation of a spherical morphology with low free energy. For the above two reasons, Cu-BTC particles are willing to nucleate spherically on the sulfonic acid SAMs template.

Table 1. N_2 adsorption constant for obtained Cu-BTC particles.

SAMs template with the ending groups	BET ($m^2 \cdot g^{-1}$)	Vmeso ($cm^3 \cdot g^{-1}$)	Pore size (nm)
blank	1323.6	0.5561	1.6801
hydroxyl-group;	1531.3	0.6328	1.6529
amino group	1606.6	0.6691	1.6658
thiol group	1660.2	0.6926	1.6687
sulfonic group;	1680.6	0.7026	1.672

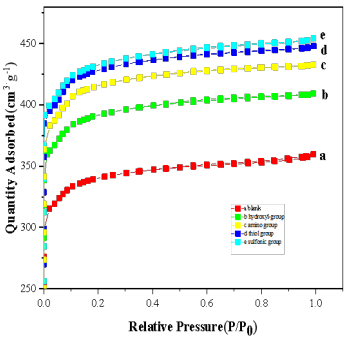

Fig.4. N_2 adsorption-isotherms of obtained Cu-BTC particles

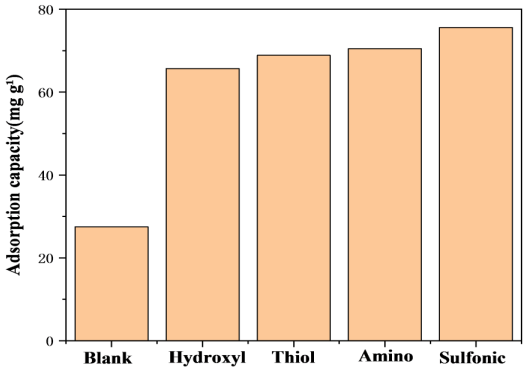

Fig 5. Adsorption capacity of MB on the Cu-BTC particles grown without template or on the template

Fig. 4 illustrates the adsorption curves of Cu-BTC samples synthesized with and without templates. The BET specific surface area, pore volume, and average pore diameter are presented in Table 1. It is evident from Fig. 4 that the adsorption of N_2 by the prepared Cu-BTC metal-organic framework materials follows a type I adsorption curve, indicating that these materials are microporous [19]. Table 1 shows that the BET specific surface area and total pore volume of the Cu-BTC sample synthesized without template induction (1323 $m^2 \cdot g^{-1}$, 0.56 $cm^3 \cdot g^{-1}$) are lower than those of the Cu-BTC synthesized with induction of self-assembled monolayers. This observation suggests that changes in morphology significantly affect the pore structure of the Cu-BTC samples. Moreover, combining these results with the SEM results indicates that the presence of more spherical particles correlates with an increased specific surface area and total pore volume of Cu-BTC. A larger specific surface area provides more active sites, thereby enhancing the superior adsorption performance.

Using MB as a model pollutant, the adsorption activity of Cu-BTC samples synthesized with and without templates was investigated. Fig.5 illustrates the adsorption capacity of samples generated without a template and those synthesized on hydroxyl substrates, as well as on amino, thiol , and sulfonic group-terminated SAMs- modified substrates. All adsorption times are 2h. The adsorption amounts of Cu-BTC in various morphologies are calculated according to equation 1.

$$q_e = \frac{V(C_0 - C_e)}{m} \quad (1)$$

where q_e is the adsorption capacity (mg g^{-1}); V is the liquid volume (L); C_0 is the initial solute concentration; C_e is the equilibrium solute concentration (mg L^{-1}); m is the amount of adsorbent (g).

As can be seen from Fig. 5, spheres nucleated on a self-organized monolayer with terminal sulfonic acid groups exhibit the highest adsorption capacity. This may be attributed to the

Table 2. Isotherm model constants for adsorption of MB dye on the Cu-BTC particles

Langmuir model			Freundlich model		
q_m/(mg g^{-1})	K_L/(L•mg^{-1})	R^2	K_F	n	R^2
141.35	0.105	0.985	28.57	2.93	0.888

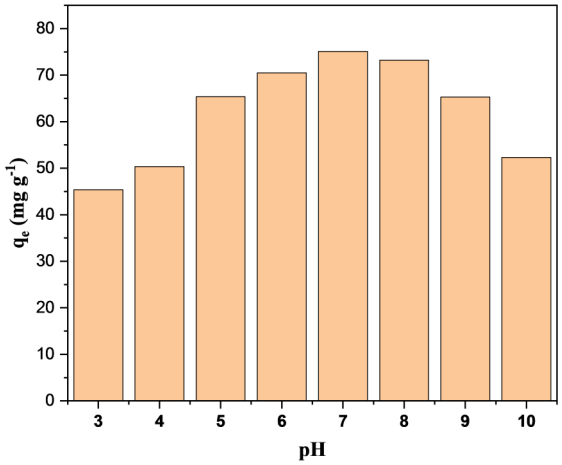

Fig. 6 Effect of the pH on Adsorption capacity of MB on the spherical Cu-BTC particles

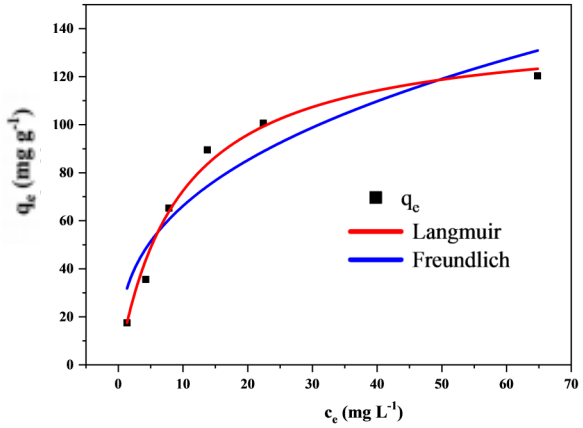

Fig. 7 Adsorption isotherms of MB dye on the spherical Cu-BTC particles.

higher specific surface area of Cu-BTC spheres, which can provide more active sites for surface reactions due to variations in particle size and stacking contact area.

As shown in Fig. 6, the adsorption effect of spherical Cu-BTC on methylene blue initially increases and then decreases with rising pH values. The degree of -COOH ionization in the Cu-BTC structure increases with an increase in pH below 7, leading to an increase in the surface negative charge of the adsorbent and enhances the electrostatic attraction between the adsorbent and methylene blue. Consequently, the adsorption efficiency of methylene blue gradually improves. In the pH range of 7 to 9, sufficient -COOH ionization on the adsorbent surface provides enough active sites for interaction; therefore, no significant change in the adsorption efficiency of methylene blue is observed. This can be attributed to enhanced electrostatic interactions between dot and methylene blue. However, when pH ranges from 9 to 10, a large amount of OH- ions are present in the sample solution causing positively charged methylene blue molecules to combine with OH-. As a result, methylene blue becomes neutralized and weakens its electrostatic interaction with the adsorbent leading to lower adsorption efficiency. Therefore, the pH value of the sample solution is chosen to be 7.

Fig. 7 illustrates the isotherm of methylene blue adsorption on spherical Cu-BTC adsorbent. In order to reveal the process and mechanism of adsorption, the data for methylene blue adsorption on Cu-BTC were fitted using the Langmuir and Freundlich isothermal adsorption models; the fitting results are presented in Table 2. The Langmuir equation (2) and the Freundlich equation (3) were employed:

$$q_e=\frac{q_m K_L C_e}{1+K_L C_e} \quad (2)$$

$$q_e=K_F C_e^{\,1/n} \quad (3)$$

where q_e is the adsorption amount at equilibrium in mg·g^{-1}; C_e is the concentration in solution at equilibrium in mg·L^{-1}; q_m is the maximum adsorption capacity in mg·g^{-1}; K_F, K_L and *n* are the adsorption constants of the Langmuir and Freundlich equations respectively.

The corresponding linear correlation coefficients (R^2) are 0.985 and 0.888, respectively. The adsorption behavior of Cu-BTC for methylene blue more closely matches the Langmuir adsorption isotherm equation, indicating that the adsorption of methylene blue by the adsorbent occurs via monolayer adsorption.

At pH 7 and the initial concentration of MB solution of 100 mg·L^{-1}, the adsorption capacity of spherical Cu-BTC changes with time, as shown in Fig. 8. At the initial stage of adsorption (during the first 40 minutes), there are numerous adsorption sites on the adsorbent

Table 3. Kinetic parameters of kinetic models for adsorption of MB dye on the spherical Cu-BTC particles

q_{exp}	The quasi first-order kinetic model			The quasi second kinetic model		
mg/g	k_1	q_{cal}	R^2	k_2	q_{cal}	R^2
75.62	0.034	75.1	0.978	0.00004	86.3	0.989

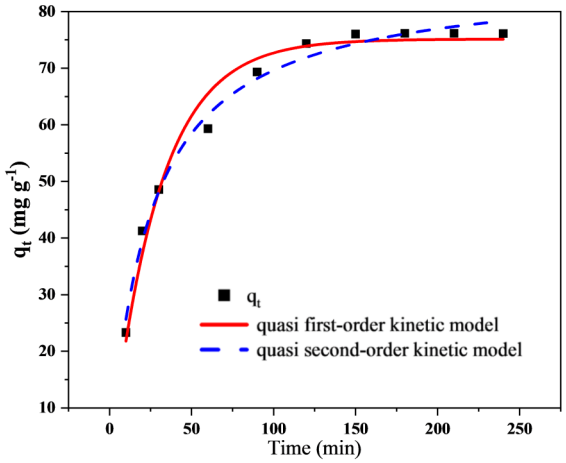

Fig. 8. (a) quasi-first-order (b) quasi -second-order plot for the adsorption of MB on the spherical Cu-BTC particles

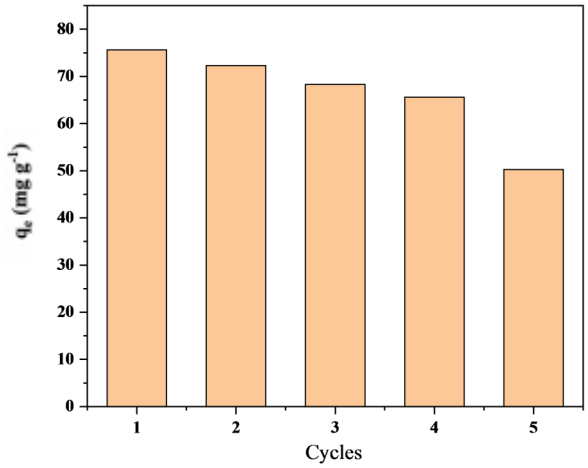

Fig. 9 Adsorption amount of MB on the spherical Cu-BTC particles in various numbers of cycles

surface, which leads to a rapid increase in adsorption capacity. Over time, the number of adsorption centers gradually approaches saturation, which leads to a slowdown in the growth of adsorption capacity. The reaction continues for 120 minutes, after which adsorption equilibrium is reached. In order to better understand the adsorption process and mechanism, the experimental data were fitted using the models of pseudo-first-order kinetics (4) and pseudo-second-order kinetics (5). The corresponding equations are as follows:

$$q_t = q_{(e,1)} \times \left(1 - e^{\frac{-k_1 t}{2.303}}\right) \quad (4)$$

$$q_t = \frac{q_{(e,2)}^2 k_2 t}{1 + k_2 q_{(e,2)} t} \quad (5)$$

where q_t and q_e are the adsorption capacity of Cu-BTC for MB at time t and at equilibrium, respectively (in mg·g^{-1}); t is the adsorption time; k_1 is the rate constant of the pseudo-first-order kinetic equation, min^{-1}; k_2 is the rate constant of the pseudo-second-order kinetic equation in g·(mg·min)$^{-1}$. The fitting results are illustrated in Fig. 8 and detailed in Table 2. The equilibrium concentration calculated using the pseudo-first-order kinetic model shows a close match with the experimental data, and its correlation coefficient (R^2 = 0.978) is impressively high, suggesting that this model is suitable for the adsorption of MB. The correlation coefficient for the pseudo-second-order kinetics, in contrast, exhibits superiority, while the fitted saturated adsorption capacity (86.3 mg·g^{-1}) significantly deviates from the measured data (75.6 mg·g^{-1}). The results indicate that the adsorption of MB by spherical Cu-BTC is physical adsorption.

An experiment utilizing spherical Cu-BTC adsorbent for the adsorption of methylene blue was conducted to evaluate the recycling capability of the adsorbent. As illustrated in Fig.9, after five adsorption cycles, the adsorption capacity of the Cu-BTC adsorbent for methylene blue decreased from 75.6 mg g^{-1} to 52.1 mg g^{-1}. However, after four adsorption cycles, the capacity of the adsorbent was 68.9 mg g^{-1}. Thus, after four cycles of reuse, Cu-BTC adsorbents retained relatively high adsorption capacity for methylene blue, indicating their promising potential for regeneration and reuse.

The high concentration of salt in dye waste water exerts a significant influence on the adsorption behavior of certain dyes. To evaluate the effect of salt on MB adsorption, we studied the adsorption capacity of Cu-BTC for MB at varying concentrations of sodium chloride. From the Fig.10, it can be seen that with increasing sodium chloride concentration, the adsorption capacity significantly decreases.

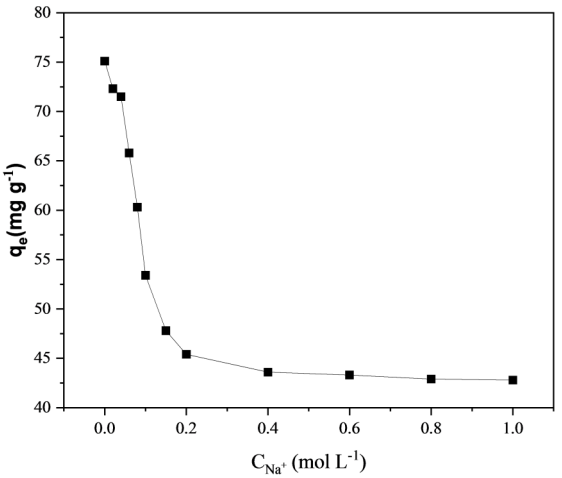

Fig. 10. Effect of NaCl concentration on the adsorption of MB on the spherical Cu-BTC particles.

Therefore, sodium chloride can inhibit the adsorption of MB on Cu-BTC particles.

4 Conclusion

We successfully prepared Cu-BTC micron structures using biomimetic mineralization technology. Self-assembled monolayer (SAM) templates were used for the nucleation and growth of Cu-BTC crystals. The morphology of the resulting structures is controlled by adjusting the end groups of templates in solution. Cu-BTC generated without template induction exhibits a typical octahedral structure, whereas the morphology produced with template induction appears spherical. Specifically, the morphology induced by sulfonic acid groups is completely spherical, and the specific surface area of the spherical Cu-BTC is significantly larger than that of the octahedral form. The increased specific surface area provides more active sites, resulting in a greater adsorption capacity for Cu-BTC generated from sulfonic acid groups compared to that generated without templates. The adsorption of methylene blue by Cu-BTC is in good agreement with the pseudo-first-order adsorption kinetic model and the Langmuir isothermal adsorption model. These results indicate that the adsorption process of methylene blue by the Cu-BTC adsorbent is characterized by single-layer adsorption, primarily governed by physical adsorption.

Acknowledgments

This research was supported by the Jilin Province Education Department project(NO.202350253)

References

1. M. Sultan, *Environ. Chem. Lett.,***347** 15 (2017).
2. Y. Song, M. Yang and X.Zhang, *Sep. Sci. Technol.,* **1521** 57 (2022).
3. V.V. Datsenko, E.B. Khobotova, *Funct. Mater.* **296** 31 **(**2024).
4. X.G. Wang, ZB. Liu, *Funct. Mater.* **377** 30 (2023) .
5. A. Ahsan, F. Jamil, M.A. et al., *Korean. J Chem. Eng.,* **2060** 40 (2024).
6. Z. N. Liu, A. Fan, C.H. Ho, *J* Environ. Eng., **04020018** 146 (2020).
7. Y. Y. Deng, X. F. Xiao, D. Wang, et al., *J Nanosci. Nanotechno.*, **1660** 20 (2020).
8. X. M. Liu, L. H. Xie and Y. F. Wu, *Inorg. Chem. Front.,***2840** 7 (2020).
9. Y. L. Liu, P. F. Gao, Y. F Li et al.,*Sci.China Chem.,* **1553** 58 (2015).
10. Q. Z. Zheng, J. H. Sheng, J. *Biomacromolecules* **5132** 24 (2023).
11. F. Lu, F B. Zhao, R.Li, et al. *J Cryst. Growth*, **33** 426 (2015).
12. F. Lu,F. F.Meng, L. L.Wang,Y. Q.Dai,*Funct. Mater.,* **54** 26,(2019).
13. R. Kaura, A. Kaura, A. Umar , *et al.*, Mater. Res. Bull.,**124** , 109(2019).
14. S.A Ban, K.Y. Long, et al., *Ind. Eng. Chem. Res* **2956** 57 (2018).
15. J.Y Lee, J. H. Choi, *Mater. Res.Exp.,* **095505** 9 (2022).
16. Y. Z. Zhu, D. P. Wu , J. H. Chen, et al., *New J.Chem.,* **3358** 46 (2022).
17. L. Addadi, S. Raz, S. Weiner, *Adv. Mater.* **959** 15 2003.
18. F.C. Meldrum, R.P. Sear, *Science*,**1802** 322 (2008).
19. K. S. W. Sing et al. *Pure and Applied Chemistry*, **603** 57 (1985).